A lattice Boltzmann scheme for a nematic–isotropic interface

2004 J. Phys.: Condens. Matter 16 S1931

(http://iopscience.iop.org/0953-8984/16/19/006)

INSTITUTE OF PHYSICS PUBLISHING JOURNAL OF PHYSICS: CONDENSED MATTER

J. Phys.: Condens. Matter **16** (2004) S1931–S1944 PII: S0953-8984(04)74289-7

A lattice Boltzmann scheme for a nematic–isotropic interface

S V Lishchuk, C M Care and I Halliday

Materials Research Institute, Sheffield Hallam University, Howard Street, S1 1WB, UK

Received 5 January 2004
Published 30 April 2004
Online at stacks.iop.org/JPhysCM/16/S1931
DOI: 10.1088/0953-8984/16/19/006

Abstract

A lattice Boltzmann (LB) model of an interface between a nematic and an isotropic fluid is presented. The method is used to study, in two dimensions, the properties of a deformable colloidal droplet of an isotropic fluid suspended in a nematic matrix. The isotropic fluid is modelled by a standard lattice Bhatnagar–Gross–Krook (LBGK) scheme. The LB model of the nematic is a modified LBGK scheme in which a tensor density is used to recover the variable order parameter nemato-dynamics scheme proposed by Qian and Sheng. The interface between the two fluids is modelled by introducing appropriate forcing at the interface. The stress balance is achieved using an extension of a method proposed by Lishchuk *et al*, and the torque balance is achieved with an appropriate surface molecular field. The resulting interface algorithm recovers the macroscopic equations developed by Rey. Results are presented for the dependence of the shape of the droplet and the nematic defects upon the surface tension and the anchoring strength. A discussion is also presented of the effect of curvature rigidity on the droplet shape.

1. Introduction

The motivation for the work presented in this paper is the development of a technique to study both the statics and dynamics of liquid crystal colloidal systems in which the colloidal particle is an isotropic fluid with a sufficiently low surface tension for deformation to be possible. It is well established that colloidal particles in a nematic matrix may introduce defects into the elastic field which lead to new interactions between colloidal particles [1]. However, the defects are difficult to describe within macroscopic theories of liquid crystals since they introduce local modifications to both the density and the order tensor (i.e. the order parameter is reduced and biaxiality is observed). The precise description of the structure and energy associated with a nematic defect is a complex problem which must be considered at a range of length scales. For this reason the study of these materials requires contributions from theories (e.g. [2–4]) and simulations (e.g. [5–7]) at the molecular, mesoscopic and continuum levels. The approach adopted in this work has the merit that it is potentially able to recover the dynamics associated

with these systems. It should be noted, however, that in this work the fluids are assumed to be incompressible.

The forces between the colloidal particles in a nematic, and the dynamics of their motion, are accessible to experiment (cf [8]). The interactions may lead to self-assembly into a range of new structures (e.g. [9–11]). There is also interest in the flow properties associated with colloidal particles embedded in a liquid crystal host [1], and the responses of the systems to external fields have also been explored [12]. Colloidal suspensions of water droplets in nematic liquid crystals have been studied experimentally [8, 13].

However, if the particle is a liquid droplet of the order of, or below, a critical size, the particle shape can distort in the nematic field and this represents a particular challenge for simulation. The critical radius is determined by the ratio of the elastic constant to the surface tension [2] and for a typical liquid crystal–surfactant–water system this is found to be of the order of 1 nm. However, if the surface tension between the nematic and isotropic phase could be significantly reduced, there arises the possibility of significant distortions at larger droplet sizes. For the inverse problem of liquid crystal droplets embedded in an isotropic matrix, distortions of the droplets to 'tactoid' and lens shapes are observed for droplets of the order of 1 μm. These latter systems have been extensively studied both experimentally and theoretically (e.g. [14–16]). However, when the nematic is the external medium, the analysis becomes complicated by the possibility of defects forming close to the surface of the droplet. In this paper, the parameters are chosen to explore the region in which the deformation of the droplets becomes important.

Director anchoring at the surface of a colloidal particle gives rise to complex defect structures. The precise behaviour of an isotropic droplet in a nematic matrix depends upon (i) the boundary conditions at the particle and the container, (ii) the elastic constants of the nematic, (iii) the anchoring energy of the nematic at the liquid interface, (iv) the size and shape of the particle, and (v), in the case of a liquid droplet, the strength of the surface tension. The balance of these properties is strongly temperature dependent and may lead to interesting phase behaviour. Poulin [17] reports that the defect structure around a droplet changes from a quadrupolar to a dipolar configuration as the temperature is reduced.

The behaviour of an isotropic droplet in a nematic matrix is controlled by the dimensionless parameters

$$\tilde{W} = \frac{WR}{K} \qquad \tilde{K} = \frac{K}{\sigma R} \qquad \tilde{\omega} = \frac{W}{\sigma} \tag{1}$$

where W is the surface anchoring strength, σ is the surface tension, K is a Frank elastic constant and R is the drop radius. We note that there are in fact only two independent dimensionless parameters, since $\tilde{\omega} = \tilde{W}\tilde{K}$. If $\tilde{K} \ll 1$, the surface tension dominates the elastic free energy. Consequently, the droplet will remain essentially spherical and the defect structure is controlled by the dimensionless anchoring strength, $\tilde{W}$. However, if $\tilde{K} \geqslant 1$, the nematic elastic energy becomes comparable, or dominates, the surface tension and the possibility of drop distortion arises. However, the distortion will only be significant for values of $\tilde{\omega} \sim 1$ where the anchoring strength is of the same order, or larger, than the surface tension. The problem becomes further complicated if we consider the curvature rigidity which may be associated with a surfactant layer on the surface of the isotropic droplet. Consideration of this effect introduces a further dimensionless parameter, $\tilde{\kappa} = \kappa/(\sigma R^2)$, which is a measure of the relative strength of the curvature rigidity to the surface tension. For systems which would otherwise exhibit a lens shape, the effect of the curvature rigidity would be to remove the sharp discontinuity in curvature.

The lattice Boltzmann (LB) method is used as the basis of the methods described to recover the results presented in section 4. The LB method has been extensively studied as a

method of simulating isotropic fluid flow (e.g. [18]). A particular strength of LB lies in its ability to model the interface between two fluids (e.g. [19–21]). In addition, a number of LB schemes have recently been developed to represent the flow of anisotropic fluids such as liquid crystals [22–24]. The goal of the work in this paper is to combine these two approaches in order to model a nematic–isotropic interface.

The paper is organized as follows. In section 2 the LB algorithm that recovers the equations for the bulk fluids is described. In section 3 the LB scheme to recover the isotropic nematic interface is described. It is used in section 4 to study a static droplet of isotropic liquid, immersed into nematic phase. The director field and the droplet shape are obtained for a range of values of the surface tension and surface anchoring parameters. In section 5 the effect of introducing a curvature rigidity are analysed. The conclusions of the paper are discussed in section 6. The appendix contains a summary of the derivation of macroscopic equations for the nematic–isotropic interface based on the arguments of Rey [25].

2. Lattice Boltzmann scheme for the bulk fluids

The results reported in this paper use an LB scheme on a two-dimensional triangular lattice with a coordination number of 13 (D2Q13) [26]. The lattice is populated by an isotropic density, f_i, and a nematic density, $g_{i\alpha\beta}$, which give the corresponding macroscopic densities, ρ^{I} and ρ^{N}. The bulk isotropic fluid is modelled with a standard, single relaxation parameter LBGK scheme [26].

In the nematic phase, the orientational ordering is characterized by a director field, $n_\alpha(\mathbf{x}, t)$, a unit vector which essentially defines the 'average orientation' of the molecules. However, the nematic ordering is more fully characterized by a traceless and symmetric order tensor, $Q_{\alpha\beta}$. For simplicity, in this work we assume that the director is confined to a two-dimensional plane, and hence that $Q_{\alpha\beta}$ may be written in the form

$$Q_{\alpha\beta}(\mathbf{x}, t) = S(2n_\alpha n_\beta - \delta_{\alpha\beta}). \tag{2}$$

The principal eigenvector of $Q_{\alpha\beta}$ is the director, and the principal eigenvalue, $S(\mathbf{x}, t)$, is the scalar order parameter. The ability to model a system with tensor order parameter is essential in order to recover the defect structure which is known for some droplet sizes.

The nematic phase is modelled using the scheme described in Care *et al* [24] which recovers the Qian–Sheng [27] equations for the flow of a nematic liquid crystal with a tensor order parameter. The scheme is based on a single LB equation which governs the evolution of the tensor density, $g_{i,\alpha\beta}$, and from which both the macroscopic order and momentum evolution equations are recovered. The equilibrium distribution function is retained as isotropic, and the anisotropy is introduced through (i) anisotropic scattering and (ii) angular and momentum forcing based on a molecular field which is derived from a Landau–deGennes free energy. The full details of the method are quite involved and will not be reported here for reasons of space; the interested reader is referred to [24].

We simply summarize here the target macroscopic equations for this LB method. The two governing equations of the Qian scheme are the momentum evolution equation

$$\rho D_t u_\beta = \partial_\beta(-P^{\mathrm{N}}\delta_{\alpha\beta} + \sigma^{\mathrm{d}}_{\alpha\beta} + \sigma^{\mathrm{f}}_{\alpha\beta} + \sigma^{\mathrm{v}}_{\alpha\beta}) \tag{3}$$

and the order tensor evolution equation

$$J\ddot{Q}_{\alpha\beta} = h^{\mathrm{e}}_{\alpha\beta} + h^{\mathrm{v}}_{\alpha\beta} - \lambda^{\mathrm{N}}\delta_{\alpha\beta} - \varepsilon_{\alpha\beta\gamma}\lambda^{\mathrm{N}}_\gamma \tag{4}$$

where $h^{\mathrm{e}}_{\alpha\beta}$ ($h^{\mathrm{v}}_{\alpha\beta}$) is the elastic (viscous) molecular field. The quantities λ^{N} and $\lambda^{\mathrm{N}}_\alpha$ are Lagrange multipliers which impose the constraints that the order tensor, $Q_{\alpha\beta}$, is symmetric and traceless in the bulk nematic.

It is shown by Qian [27] that in the limit of constant order parameter, the solutions of these equations is identical to those obtained from the standard Ericksen–Leslie–Parodi equations [28]. We use the repeated index notation for summations over Cartesian indices. In the above equations, $D_t = \partial_t + u_\mu \partial_\mu$ is the convective derivative, and P^{N} is the pressure in the nematic phase. $\sigma^{\mathrm{v}}_{\alpha\beta}$ is the viscous stress tensor

$$\sigma^{\mathrm{v}}_{\alpha\beta} = \beta_1 Q_{\alpha\beta} Q_{\mu\nu} A_{\mu\nu} + \beta_4 A_{\alpha\beta} + \beta_5 Q_{\alpha\mu} A_{\mu\beta} + \beta_6 Q_{\beta\mu} A_{\mu\alpha} + \tfrac{1}{2}\mu_2 N_{\alpha\beta} - \mu_1 Q_{\alpha\mu} N_{\mu\beta} + \mu_1 Q_{\beta\mu} N_{\mu\alpha} \tag{5}$$

where $A_{\alpha\beta} = \frac{1}{2}(\partial_\alpha u_\beta + \partial_\beta u_\alpha)$ is the symmetric velocity gradient tensor, and $N_{\alpha\beta}$ is the co-rotational derivative defined by $N_{\alpha\beta} = \partial_t Q_{\alpha\beta} + u_\mu \partial_\mu Q_{\alpha\beta} - \varepsilon_{\alpha\mu\nu}\omega_\mu Q_{\nu\beta} - \varepsilon_{\beta\mu\nu}\omega_\mu Q_{\nu\alpha}$ with ω_μ being the fluid vorticity. In equation (5), $\sigma^{\mathrm{d}}_{\alpha\beta}$ is the distortion stress tensor

$$\sigma^{\mathrm{d}}_{\alpha\beta} = -\frac{\partial f^{\mathrm{N}}}{\partial(Q_{\mu\nu,\alpha})} Q_{\mu\nu,\beta} \tag{6}$$

where $Q_{\alpha\beta,\gamma} \equiv \partial_\gamma(Q_{\alpha\beta})$ and $\sigma^{\mathrm{f}}_{\alpha\beta}$ is the stress tensor associated with an externally applied field. The bulk elastic molecular field is given by

$$h^{\mathrm{e}}_{\alpha\beta} = -\frac{\partial f^{\mathrm{N}}}{\partial Q_{\alpha\beta}} + \partial_\mu \frac{\partial f^{\mathrm{N}}}{\partial(Q_{\alpha\beta,\mu})} \tag{7}$$

where we assume the free energy density of the bulk nematic, f^{N}, is given by a Landau–deGennes expression of the form

$$f^{\mathrm{N}} = f^{\mathrm{Nh}} + f^{\mathrm{Ng}} \tag{8}$$

where the homogeneous contribution, f^{Nh}, is given by

$$f^{\mathrm{Nh}} = \tfrac{1}{2}(\alpha_F Q^2_{\mu\nu} - \beta_F Q_{\mu\nu} Q_{\nu\tau} Q_{\tau\mu} + \gamma_F (Q^2_{\mu\nu})^2) \tag{9}$$

and the gradient contribution, f^{Ng}, is given by

$$f^{\mathrm{Ng}} = \tfrac{1}{2}(L_1 Q^2_{\mu\nu,\tau} + L_2 Q_{\mu\nu,\nu} Q_{\mu\tau,\tau}). \tag{10}$$

Using this form of the free energy the bulk molecular field, equation (7), is given by

$$h^{\mathrm{e}}_{\alpha\beta} = L_1 \partial^2_\mu Q_{\alpha\beta} + L_2 \partial_\beta \partial_\mu Q_{\alpha\mu} - \alpha_F Q_{\alpha\beta} + 3\beta_F Q_{\alpha\mu} Q_{\beta\mu} - 4\gamma_F Q_{\alpha\beta} Q^2_{\mu\nu}. \tag{11}$$

3. Lattice Boltzmann algorithm for a nematic–isotropic interface

There have been a number of theoretical studies of the interface between an isotropic and a nematic fluid [15, 25, 29, 30]. At such an interface it is necessary to satisfy a torque balance equation and a momentum balance equation. The bulk LB technique described in [24] may be developed to recover the macroscopic equations proposed by Rey [25, 29] for such an interface. However, the surface free energy (which gives the surface molecular field and a surface stress tensor) depends upon an impracticably large number of parameters. These include anchoring coefficients which control the nature of the static interface and a large number of surface viscosity coefficients. Only a limited number of these parameters are included in this work.

In a recent article, [31], the authors reported a method of obtaining a surface tension at the interface between two isotropic fluids by introducing a forcing term on the mixed (surface) sites which is dependent on the surface curvature; the segregation of the two fluids is maintained by the technique of Gunstensen [19]. The method [31] significantly reduces the micro-currents which are an artefact observed in most LB interface schemes.

It is possible to combine the scheme for the bulk nematic phase described above with the interface scheme [31] to recover a nematic–isotropic interface based on the continuum

description proposed by Rey [25, 29]. The key additional feature to recover the nematic–isotropic interface is the introduction of a surface molecular field and a surface stress tensor. A surface unit normal, k_α, is constructed from the gradient of the nematic density at mixed sites, $\phi_\alpha = \partial_\alpha(\rho^{\mathrm{N}}/\rho)$. The surface normal is used to calculate an elastic surface molecular field

$$h^{\mathrm{S}}_{\alpha\beta} = -Wk_\alpha k_\beta - L_1 k_\mu \partial_\mu Q_{\alpha\beta} - L_2 k_\alpha \partial_\mu Q_{\mu\beta} \tag{12}$$

and an elastic surface stress tensor

$$\sigma^{\mathrm{S}}_{\alpha\beta} = \sigma(\delta_{\alpha\beta} - k_\alpha k_\beta) + W[\delta_{\alpha\beta} Q_{\mu\nu} k_\mu k_\nu + Q_{\mu\nu} k_\mu k_\nu k_\alpha k_\beta - 2Q_{\alpha\mu} k_\mu k_\beta] \tag{13}$$

where σ controls the strength of the surface tension, W controls the anchoring strength, and $\{L_1, L_2\}$ control the elastic constants of the nematic. The results (12) and (13) follow from a surface free energy density equivalent to that proposed by Rapini [32]. A summary of the origin of equations (12) and (13) is given in the appendix. The viscous contributions to the surface molecular field and surface stress tensor are not included since we are only interested in this work in the steady state solutions.

In order to generate an isotropic–nematic interface, the forcing introduced in [31] is adapted to give a forcing for the nematic surface densities of the form

$$\phi^{\mathrm{N}}_{i\alpha\beta} = \frac{\rho^{\mathrm{N}}}{\rho} S_{\alpha\beta} \phi^{\mathrm{S}}_i \tag{14}$$

and, for the isotropic surface densities,

$$\phi^{\mathrm{I}}_i = \frac{\rho^{\mathrm{I}}}{\rho} \phi^{\mathrm{S}}_i \tag{15}$$

where

$$\phi^{\mathrm{S}}_i = \frac{1}{c_s^2} t_i c_{i\mu} |\phi| \partial^{\mathrm{S}}_\nu \sigma^{\mathrm{S}}_{\nu\mu} \tag{16}$$

with the surface gradient defined by

$$\partial^{\mathrm{S}}_\alpha = (\delta_{\alpha\beta} - k_\alpha k_\beta)\partial_\beta. \tag{17}$$

The angular forcing in the LB algorithm is modified on the surface sites to include a contribution from the surface molecular field

$$\chi_{i\alpha\beta} = t_i \rho^{\mathrm{N}} \left\{ (\varepsilon_{\alpha\nu\mu} Q_{\beta\mu} + \varepsilon_{\beta\nu\mu} Q_{\alpha\mu})\omega_\nu - \frac{1}{2\mu_1}[\mu_2 A_{\alpha\beta} - 2(h_{\alpha\beta} + |\phi| h^{\mathrm{S}}_{\alpha\beta}) + 2\delta_{\alpha\beta}\lambda + 2\varepsilon_{\alpha\beta\mu}\lambda_\mu] \right\}. \tag{18}$$

The segregation of the two fluids is achieved using the method of Gunstensen [19], but it is important to note that the surface tension inducing perturbation used by Gunstensen is replaced by the forcing described in the previous paragraph.

4. Results

In this section we report results obtained by applying the technique presented in sections 2 and 3 to explore the behaviour of a droplet of an isotropic fluid embedded in a nematic liquid crystal. The results are for steady state solutions; the effect of introducing flow fields will be explored in a future publication.

The effect of modifying the surface tension, σ, and the anchoring strength, W, is illustrated in figure 1 for a system with homeotropic alignment on the surface of the drop. The picture is a collage of six separate simulations in which the free energy parameters controlling the elastic constants are fixed at the values $L_1 = 10^{-4}$ and $L_2 = 0$. Each simulation was run to steady

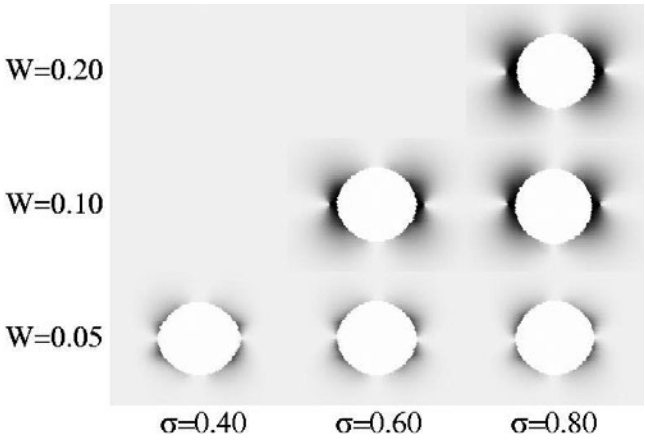

Figure 1. Steady state droplets for various values of the anchoring strength, W, and surface tension, σ.

state on a 200×200 grid with the droplet being initialized as a disc with a diameter of 48 sites. Periodic boundary conditions were imposed in which the director was aligned perpendicular to the top and bottom surfaces. The grey scale is used to represent the direction of the director, with white (black) corresponding to the director aligned vertically (horizontally).

It can be seen that the droplet becomes more circular with increasing surface tension, σ, as would be expected. From the arguments used for solid colloidal particles [1] it is expected that the position of the defects will be controlled by the dimensionless quantity $\tilde{W} = WR/K$, where R is an average drop radius. In the results presented here, the nematic elastic constant and drop size are fixed and hence the parameter $\tilde{W}$ is controlled simply by W. If we consider the set of drops with $\sigma = 0.8$, it can be seen that for small values of W there are no defects, and the nematic field distorts to become tangentially oriented at the equator of the sphere. As W increases, two defects become detached from the droplet, forming a structure which is equivalent to the Saturn ring observed around three-dimensional colloidal spheres.

Figure 2 shows a sequence of simulations with the surface tension, σ, fixed at 0.9 and with varying surface anchoring parameter, W. It can be seen that the position of the defect jumps from the surface at a value for W which lies between 0.09 and 0.1.

Figure 3 shows the effect of changing the surface tension with the anchoring strength fixed at $W = 0.05$. As σ is reduced the droplet becomes distorted from its circular shape. Since the director field is not strongly distorted throughout this range, the system is equivalent to the inverse case of a nematic droplet, with a homogeneous director field, embedded in an isotropic matrix. Prinsen *et al* [16] predicted that the aspect ratio for this system should behave as $1 + W/\sigma$ and the results can be seen to be in good agreement with this prediction (solid curve).

In figure 4 the surface tension is changed while keeping $W/\sigma = 0.1$, and it can be seen that the data are in agreement with the predictions of [16] that the aspect ratio should behave as $1 + W/\sigma$ for a uniform director field.

For larger values of W and smaller values of σ (e.g. $\sigma = 0.4$, $W = 0.2$) the drop initially distorts to a well defined elongated shape equivalent to a lens in three dimensions, shown schematically in figure 5(a). Increasing the surface tension on this distorted shape produces a jump to a defect structure as illustrated schematically in figure 5(b). However, at very long times these highly deformed structures become unphysically distorted and this is associated with increased microcurrent activity. It is thought that the problem arises because of the

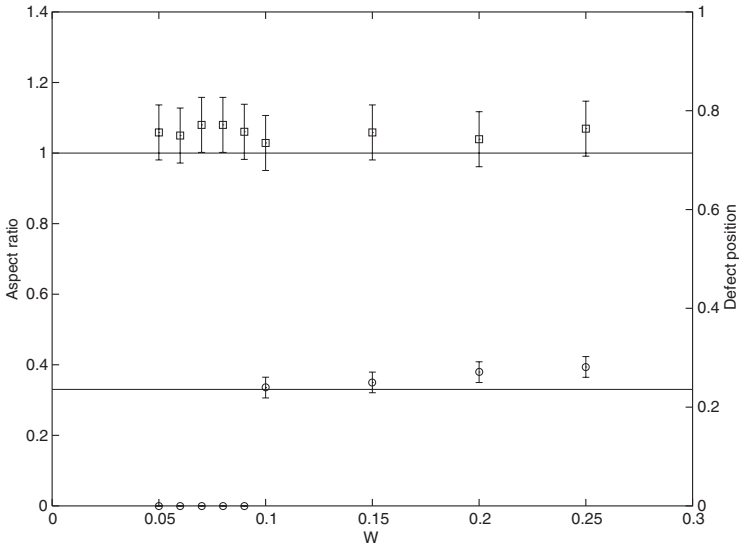

Figure 2. Droplet aspect ratio (top data) and defect position (lower data) as a function of anchoring coefficient, W, for $\sigma = 0.9$.

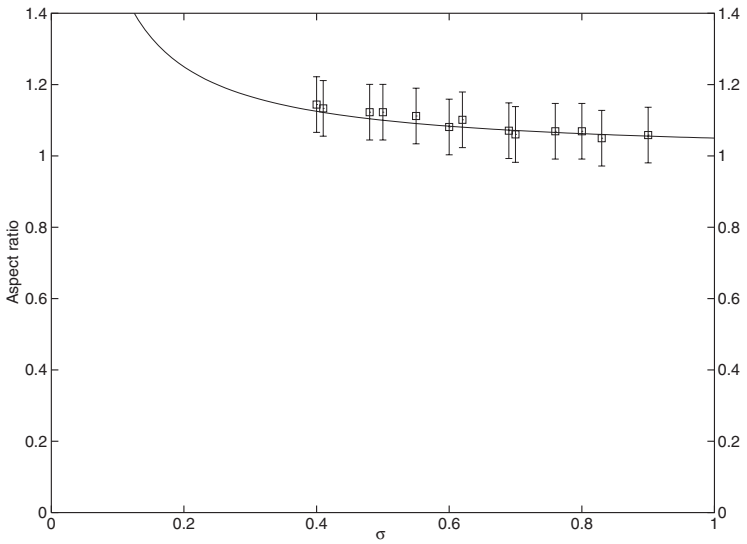

Figure 3. Droplet aspect ratio as a function of surface tension, σ, for $W = 0.05$.

numerical problem of calculating the surface gradient close to the apex of the lens structure. Results are therefore unreliable in this region, although the results do suggest that highly elongated structures may be observed for these values of the anchoring strength and surface tension.

5. The effect of curvature rigidity

In the previous section it was found that the LB algorithm experienced numerical difficulties at the points where there were large curvatures. It is therefore of interest to determine the length scales over which the curvature changes rapidly, and this will be controlled by the curvature

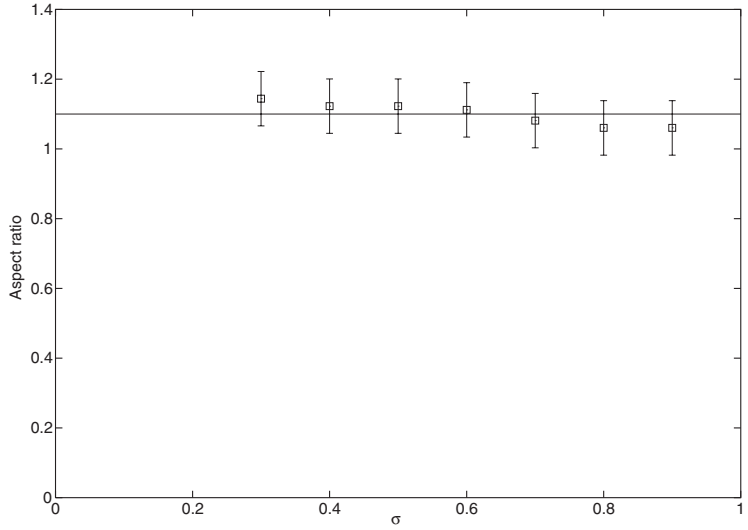

Figure 4. Droplet aspect ratio as a function of surface tension, σ, with $W/\sigma = 0.1$.

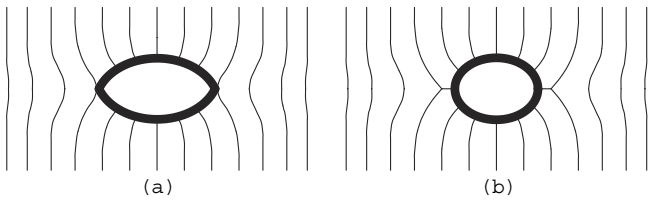

Figure 5. A schematic illustration of the nematic field around a droplet (a) before and (b) after the formation of defects.

rigidity of the surface. In this section we therefore present a preliminary analysis of the effect of curvature rigidity on the nematic–isotropic interface by direct consideration of the free energy of the droplet.

If we consider a lens shaped droplet in three dimensions and assume that the radius of curvature at the edge of the lens is δ, the energy associated with the apex of the lens will be proportional to $\kappa R/\delta$, where R is the radius of the lens and κ is the curvature rigidity associated with the surface. It can be seen that this term will become the dominant free energy contribution as the radius curvature at the edge of the lens, δ, becomes sufficiently small. It should be noted, however, that for a tactoid shape [16], the contribution of the curvature energy does not diverge because the singularity in the curvature is confined to two points.

In order to understand the effect of curvature rigidity, we consider the problem of an isotropic droplet placed in a nematic with the director aligned uniformly in the z direction, as shown in figure 6.

We therefore ignore the free energy contribution from distortion in the director field around the droplets which would be expected to be observed experimentally. This problem is essentially equivalent to that considered by Prinsen *et al* [16] of a nematic droplet with a uniform director field embedded in an isotropic fluid.

There are number of possible coordinate systems which can be used to describe the surface of the droplet, each of which leads to an alternative form of the Euler-Lagrange equations

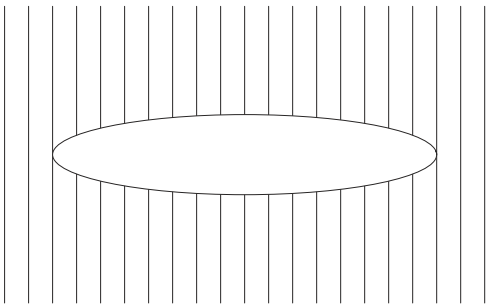

Figure 6. The uniform director field around a droplet.

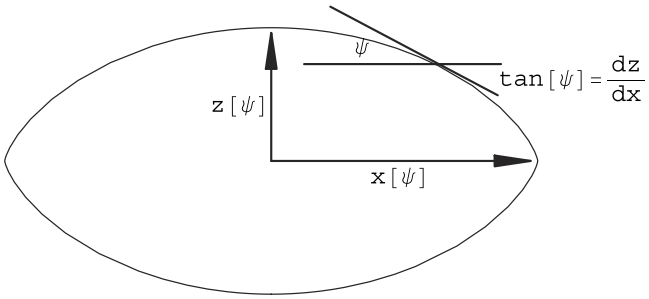

Figure 7. The coordinate definition for a droplet surface.

and the boundary conditions which must be satisfied by the variables. We use here the representation which is shown in figure 7. In terms of this coordinate system the free energy of the droplet is given by

$$L = 2\pi \int_0^{\pi} \mathrm{d}\psi\, x'(\psi)x(\psi)[W\cos\psi + K(C_1^2 + C_2^2)^2 \sec\psi + 2\sigma\sec\psi - \lambda x(\psi)\tan\psi] \quad (19)$$

where W is the anchoring energy, K is a the curvature energy, σ is the surface tension, and λ is a Lagrange multiplier to enforce the constraint that the volume of the droplet is constant. Given this form of the free energy it is straightforward to derive the associated Euler-Lagrange equation

$$\sin\psi(1 - \omega\cos^2\psi) - \lambda x(\psi) = \kappa\left[-2\frac{\cos^2\psi\sin\psi}{x(\psi)^2} - \frac{\sin^3\psi}{x(\psi)^2} - \frac{\cos^2\psi\sin\psi}{x'(\psi)^2} + 2\frac{\cos^3\psi}{x(\psi)x'(\psi)} - 2\frac{x''(\psi)\cos^3\psi}{x'(\psi)^3}\right]. \quad (20)$$

This is a second order ordinary differential equation with the two boundary conditions $\{x(0) = 0; x(\pi) = 0\}$ which are required to achieve a closed surface with the required symmetry.

If we set κ to zero in (20), we recover an algebraic equation for $x(\psi)$ which is equivalent to that derived by Prinsen *et al* [16]. However, obtaining solutions to the Euler-Lagrange equation for small, but non-zero, values of κ presents considerable difficulties, even numerically. Thus, the presence of a small parameter pre-multiplying the highest derivative, $x''(\psi)$, leads to a form of singular perturbation problem (e.g. [33]) which prevents straightforward perturbation expansions in terms of the parameter κ. The alternative coordinate systems which were explored did not overcome this difficulty. The problem of obtaining a numerical solution

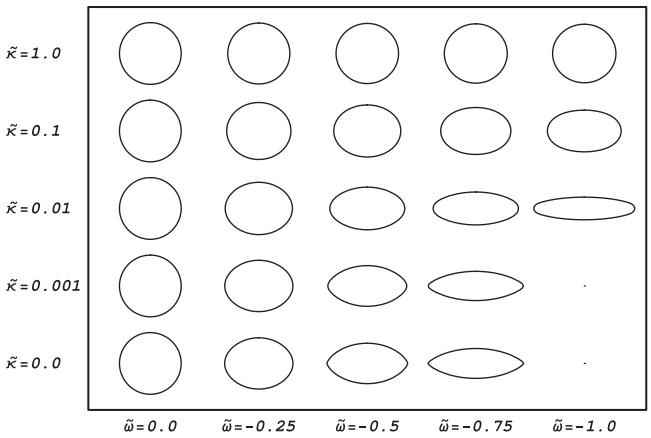

Figure 8. Cross sections of three-dimensional droplets which minimize the free energy given by equation (19).

of (20) is compounded by singularities at the boundaries which essentially arise when the equation is inverted to obtain a numerical expression for $x''(\psi)$.

In order to make progress, the free energy was minimized directly for a three-dimensional system, without recourse to the Euler-Lagrange equation. A Fourier expansion of $x(\psi)$ was constructed with the coefficients scaled to enforce a constant drop volume. Figure 8 shows the droplet shapes obtained for a range of values of the dimensionless parameter $\tilde{\omega}$ defined in equation (1) and the dimensionless curvature rigidity, $\tilde{\kappa} = \kappa/(\sigma R^2)$, where R is the undistorted droplet radius. The elements of the array in the figure which do not include a diagram correspond to values of the parameters for which the numerical solver failed to converge. The bottom row, with $\tilde{\kappa} = 0$, corresponds to the results predicted by Prinsen [16], with a lens shape forming for $\tilde{\omega} > 0.5$.

It can be seen that as the curvature rigidity increases, the drop shape becomes less curved at the perimeter of the lens, as would be expected. Indeed if we assume a value of $\sigma = 10^{-2}$ N m^{-1}, which is typical of a water–surfactant–oil interface, and a value of $\kappa = 10^{-21}$ J typical of a microemulsion [34], the droplets in the figure with $\tilde{\kappa} = 0.1$ corresponds to droplets with $R = 1$ nm. This is also the droplet size for these systems at which distortion of the droplet is expected to be observed. The effects of the curvature rigidity would be observable for larger droplets if the surface tension were reduced or the rigidity increased. Thus if experimental systems can be identified for which $\sigma = 10^{-6}$ N m^{-1}, the line $\kappa = 0.1$ corresponds to droplets of 1 μm. These arguments suggest that the LB method must be extended to include the effect of surface rigidity if it is correctly to describe the distortion of isotropic droplets in a nematic matrix.

6. Discussion and conclusions

An LB method for simulating a nematic–isotropic interface has been reported, and the method is constructed to recover the macroscopic scheme proposed by Rey [25]. The technique has been used to study the steady state behaviour of a single isotropic droplet embedded in a nematic matrix. For large values of the surface tension, the droplets exhibit only small distortion, and defects are observed to form at some critical value of the anchoring strength. The appearance of the defects is associated with increased isotropy of the droplet.

As the surface tension is reduced, the droplet becomes more distorted. For low values of the anchoring strength the results are in good agreement with the predictions for the inverse problems discussed by Prinsen [16]. With increasing anchoring strength at low surface tension values the curvature of the droplets becomes larger. However, these more extreme shapes lead to numerical instabilities arising from the difficulties in calculating surface gradients. The effect of curvature rigidity on the droplet shape was analysed by direct minimization of the free energy. It was found that the effect of curvature rigidity would need to be included in any model in which large curvatures were obtained.

Future work will focus on attempting to reduce the numerical instabilities and also to move to modelling the droplets in a flow field.

Acknowledgments

The authors would like to thank Dr Doug Cleaver and Dr Alejandro Rey for valuable discussions, and the Engineering and Physical Sciences Research Council (Grant Ref: GR/R41170/01) for the financial support of SVL.

Appendix. Theory of the isotropic–nematic interface

In this section we set out the target equations which describe the isotropic–nematic interface which must be recovered by the LB scheme. In particular, we derive the expressions used in the LB scheme for the elastic surface molecular field (12) and the surface stress tensor (13), following closely the presentation of Rey [25, 29].

The nematic–isotropic interface is characterized by a unit normal, **k**, directed from the nematic phase into the isotropic phase. Its mean Gaussian curvature is given by

$$H = -\tfrac{1}{2}\partial^{\mathrm{S}}_{\alpha} k_{\alpha}, \tag{21}$$

where the surface gradient operator is defined by

$$\partial^{\mathrm{S}}_{\alpha} = I^{\mathrm{S}}_{\alpha\beta}\partial_{\beta} \tag{22}$$

with

$$I^{\mathrm{S}}_{\alpha\beta} = \delta_{\alpha\beta} - k_{\alpha}k_{\beta}. \tag{23}$$

The divergence of $I^{\mathrm{S}}_{\alpha\beta}$ gives the surface normal vector

$$\partial^{\mathrm{S}}_{\alpha} I^{\mathrm{S}}_{\alpha\beta} = 2Hk_{\beta}. \tag{24}$$

The total free energy, F, of the nematic is given in terms of the bulk free energy density, f^{N}, and the surface free energy density, f^{S}, by

$$F = \int f^{\mathrm{N}}\,\mathrm{d}V + \int f^{\mathrm{S}}\,\mathrm{d}S \tag{25}$$

where the f^{N} was defined in equation (8) and the surface free energy density f^{S} is given in terms of the sum of isotropic and anchoring contributions:

$$f^{\mathrm{S}} = f^{\mathrm{Si}} + f^{\mathrm{Sa}} \tag{26}$$

where

$$f^{\mathrm{Si}} = \beta_{00}, \tag{27}$$

β_{00} being the isotropic interfacial surface tension parameter, and

$$f^{\mathrm{Sa}} = \beta_{11}k_{\mu}Q_{\mu\nu}k_{\nu} + \beta_{20}Q_{\mu\nu}Q_{\nu\mu} + \beta_{21}k_{\mu}Q_{\mu\nu}Q_{\nu\kappa}k_{\kappa} + \beta_{22}(k_{\mu}Q_{\mu\nu}k_{\nu})^2 \tag{28}$$

where $\{\beta_{ij}\}$, $ij = 11, 20, 21, 22$, are the anchoring coefficients.

The interfacial torque balance equation is

$$h^{\mathrm{Se}}_{\alpha\beta} + h^{\mathrm{Sv}}_{\alpha\beta} - \lambda^{\mathrm{S}}\delta_{\alpha\beta} - \varepsilon_{\alpha\beta\mu}\lambda^{\mathrm{S}}_{\mu} = 0. \tag{29}$$

Here λ^{S} and $\lambda^{\mathrm{S}}_{\mu}$ are the Lagrange multipliers determined by requirements that the order tensor is traceless and symmetric. The surface elastic molecular field is

$$h^{\mathrm{Se}}_{\alpha\beta} = -\frac{\partial f^{\mathrm{S}}}{\partial Q_{\alpha\beta}} + \partial^{\mathrm{S}}_{\mu}\left(\frac{\partial f^{\mathrm{S}}}{\partial(\partial^{\mathrm{S}}_{\mu}Q_{\alpha\beta})}\right) - k_{\mu}\left(\frac{\partial f^{B}}{\partial Q_{\alpha\beta,\mu}}\right) \tag{30}$$

and $h^{\mathrm{Sv}}_{\alpha\beta}$ is the surface viscous molecular field. The interfacial stress balance equation is

$$k_{\mu}(\sigma^{\mathrm{N}}_{\mu\alpha} - \sigma^{\mathrm{I}}_{\mu\alpha}) = \partial^{\mathrm{S}}_{\mu}\sigma^{\mathrm{Se}}_{\mu\alpha} + \partial^{\mathrm{S}}_{\mu}\sigma^{\mathrm{Sv}}_{\mu\alpha}. \tag{31}$$

Here, $\sigma^{\mathrm{N}}_{\alpha\beta}$ is the total bulk stress tensor in the nematic phase

$$\sigma^{\mathrm{N}}_{\alpha\beta} = -P^{\mathrm{N}}\delta_{\alpha\beta} + \sigma^{\mathrm{d}}_{\alpha\beta} + \sigma^{\mathrm{f}}_{\alpha\beta} + \sigma^{\mathrm{v}}_{\alpha\beta} \tag{32}$$

and $\sigma^{\mathrm{I}}_{\alpha\beta} = -P^{\mathrm{I}}\delta_{\alpha\beta} + \sigma^{Iv}_{\alpha\beta}$ is the total bulk stress tensor in the isotropic phase, $\sigma^{Iv}_{\alpha\beta}$ being the viscous stress tensor in the isotropic phase. σ^{Se} is the total elastic surface stress tensor

$$\sigma^{\mathrm{Se}}_{\alpha\beta} = I^{\mathrm{S}}_{\alpha\beta}f^{\mathrm{S}} - I^{\mathrm{S}}_{\alpha\mu}\left(\frac{\partial f^{\mathrm{S}}}{\partial k_{\mu}}k_{\beta}\right) - I^{\mathrm{S}}_{\alpha\kappa}\left(\frac{\partial f^{\mathrm{S}}}{\partial(\partial^{\mathrm{S}}_{\kappa}Q_{\mu\nu})}\right)\partial^{\mathrm{S}}_{\beta}Q_{\mu\nu} \tag{33}$$

and σ^{Sv} is the viscous surface stress tensor. The quantities $h^{\mathrm{Sv}}_{\alpha\beta}$ and σ^{Sv} are not needed in this work since we are only considering steady state systems.

The surface elastic molecular field (30) can be cast as the sum of anchoring and gradient contributions:

$$h^{\mathrm{Se}}_{\alpha\beta} = h^{\mathrm{Sea}}_{\alpha\beta} + h^{\mathrm{Seg}}_{\alpha\beta} \tag{34}$$

where, after substitution from equations (10) and (28), we find

$$h^{\mathrm{Sea}}_{\alpha\beta} = -\beta_{11}k_{\alpha}k_{\beta} - 2\beta_{20}Q_{\alpha\beta} - 2\beta_{21}k_{\mu}(Q_{\mu\beta}k_{\alpha} + Q_{\mu\alpha}k_{\beta}) - 2\beta_{22}k_{\alpha}k_{\beta}k_{\mu}k_{\nu}Q_{\mu\nu} \tag{35}$$

and

$$h^{\mathrm{Seg}}_{\alpha\beta} = -L_1 k_{\mu}\partial_{\mu}Q_{\alpha\beta} - L_2 k_{\alpha}\partial_{\mu}Q_{\mu\beta}. \tag{36}$$

The elastic surface stress tensor (33) is given by the sum of the normal σ^{Sne} and bending σ^{Sbe} stresses:

$$\sigma^{\mathrm{Se}}_{\alpha\beta} = \sigma^{\mathrm{Sne}}_{\alpha\beta} + \sigma^{\mathrm{Sbe}}_{\alpha\beta} \tag{37}$$

where with the help of (26)–(28), the normal elastic surface stress tensor is given by

$$\sigma^{\mathrm{Sne}}_{\alpha\beta} = I^{\mathrm{S}}_{\alpha\beta}[\beta_{00} + \beta_{11}k_{\mu}Q_{\mu\nu}k_{\nu} + \beta_{20}Q_{\mu\nu}Q_{\mu\nu} + \beta_{21}k_{\mu}Q_{\mu\nu}Q_{\nu\kappa}k_{\kappa} + \beta_{22}(k_{\mu}Q_{\mu\nu}Q_{\nu\kappa}k_{\kappa})^2] \tag{38}$$

and the bending elastic surface stress tensor is given by

$$\sigma^{\mathrm{Sbe}}_{\alpha\beta} = -2\beta_{11}I^{\mathrm{S}}_{\alpha\mu}Q_{\mu\nu}k_{\nu}k_{\beta} - 2\beta_{21}I^{\mathrm{S}}_{\alpha\mu}Q_{\mu\nu}Q_{\nu\kappa}k_{\kappa}k_{\beta} - 4\beta_{22}(Q_{\mu\nu}k_{\mu}k_{\nu})I^{\mathrm{S}}_{\alpha\mu}Q_{\mu\nu}k_{\nu}k_{\beta}. \tag{39}$$

The net elastic surface force G^{Se}_{α} is given by the surface gradient of the elastic surface stress tensor:

$$G^{\mathrm{Se}}_{\alpha} = \partial^{\mathrm{S}}_{\mu}\sigma^{\mathrm{S}}_{\mu\alpha}. \tag{40}$$

The normal stress σ^{Sne} and the bending stress σ^{Sbe} contribute to the net surface force. The normal stress σ^{Sne} generates tangential Marangoni force caused by surface gradients of the

tensor order parameter and independent of curvature, and the usual normal force existing due to the presence of curvature:

$$G_\alpha^{\mathrm{Sne}} = \partial_\alpha^{\mathrm{S}} f^{\mathrm{S}} - K f^{\mathrm{S}} k_\alpha. \tag{41}$$

The bending stress σ^{Sb} generates both normal and tangential components of the force existing due to anisotropic surface tension of nematics:

$$G_\alpha^{\mathrm{Sbe}} = k_\alpha (K k_\mu - \partial_\mu^{\mathrm{S}}) \frac{\partial f^{\mathrm{S}}}{\partial k_\mu} - \left(\frac{\partial f^{\mathrm{S}}}{\partial k_\mu} \partial_\mu^{\mathrm{S}} \right) k_\alpha. \tag{42}$$

If we retain only terms up to the first order in $\mathbf{Q}$ in the surface free energy density (28), we obtain the expression

$$f^{\mathrm{S}} = \beta_{00} + \beta_{11} k_\mu Q_{\mu\nu} k_\nu, \tag{43}$$

that can be shown to give the expression for surface free energy proposed by Rapini [32]. The elastic surface molecular field and the elastic surface stress tensor corresponding to this expression for the surface free energy density are given by

$$h_{\alpha\beta}^{\mathrm{Se}} = -\beta_{11} k_\alpha k_\beta - L_1 k_\mu \partial_\mu Q_{\alpha\beta} - L_2 k_\alpha \partial_\mu Q_{\mu\beta} \tag{44}$$

and

$$\sigma_{\alpha\beta}^{\mathrm{Se}} = \beta_{00}(\delta_{\alpha\beta} - k_\alpha k_\beta) + \beta_{11}[\delta_{\alpha\beta} Q_{\mu\nu} k_\mu k_\nu + Q_{\mu\nu} k_\mu k_\nu k_\alpha k_\beta - 2 Q_{\alpha\mu} k_\mu k_\beta]. \tag{45}$$

These last two expressions are equations (12) and (13) of section 3.

References

[1] Stark H 2001 *Phys. Rep.* **351** 387–474
[2] Lubensky T C, Pettey D, Currier N and Stark H 1998 *Phys. Rev.* E **57** 610
[3] Lev B I and Tomchuk P M 1999 *Phys. Rev.* E **59** 591
[4] Fukuda J Y 2002 *Phys. Rev.* E **66** 012703
[5] Ruhwandl R W and Terentjev E M 1997 *Phys. Rev.* E **56** 5561
[6] Andrienko D, Germano G and Allen M 2001 *Phys. Rev.* E **63** 041701
[7] Yamamoto R 2001 *Phys. Rev. Lett.* **87** 075502
[8] Poulin P, Cabuil V and Weitz D A 1997 *Phys. Rev. Lett.* **79** 4682
[9] Poulin P and Weitz D A 1998 *Phys. Rev.* E **57** 626
[10] Anderson V J, Terentjev E M, Meeker S P, Crain J and Poon W C K 2001 *Eur. Phys. J.* E **4** 11
[11] Petrov P G and Terentjev E M 2001 *Langmuir* **17** 2942
[12] Park C S, Clark N A and Noble R D 1994 *Phys. Rev. Lett.* **72** 1838
[13] Loudet J C, Barois P and Poulin P 2000 *Nature* **407** 611
[14] Herring C 1951 *Phys. Rev.* **82** 87
[15] Virga E 1994 *Variational Theories for Liquid Crystals* (London: Chapman and Hall)
[16] Prinsen P and van der Schoot P 2003 *Phys. Rev.* E **68** 021701
[17] Poulin P 2002 private communication
[18] Succi S 2001 *The Lattice Boltzmann Equation for Fluid Mechanics and Beyond* (Oxford: Oxford University Press)
[19] Gunstensen A K, Rothman D H, Zaleski S and Zanetti G 1991 *Phys. Rev.* A **43** 4320
[20] Swift M R, Orlandini E, Osborn W R and Yeomans J M 1996 *Phys. Rev.* E **54** 5041
[21] Halliday I, Thompson S P and Care C M 1998 *Phys. Rev.* E **57** 514
[22] Care C M, Good K and Halliday I 2000 *J. Phys.: Condens. Matter* **12** L665
[23] Denniston C, Orlandini E and Yeomans J M 2001 *Phys. Rev.* E **63** 056702
[24] Care C M, Halliday I, Good K and Lishchuk S V 2003 *Phys. Rev.* E **67** 061703
[25] Rey A D 2001 *Liq. Cryst.* **28** 549
[26] Qian Y H, d'Humieres D and Lallemand P 1992 *Europhys. Lett.* **17** 479
[27] Qian T and Sheng P 1998 *Phys. Rev.* E **58** 7475
[28] deGennes P G and Prost J 1993 *The Physics of Liquid Crystals* 2nd edn (Oxford: Clarendon)
[29] Rey A D 2000 *Phys. Rev.* E **61** 1540–9

[30] Sluckin T J and Poniewierski A 1986 *Fluid Interfacial Phenomena* (Chichester: Wiley) chapter 5
[31] Lishchuk S V, Care C M and Halliday I 2003 *Phys. Rev.* E **67** 036701
[32] Sonin A A 1995 *The Surface Physics of Liquid Crystals* (London: Gordon and Breach)
Rapini A and Papoular M 1969 *J. Physique Coll.* **30** C4–54
[33] Jordan D W and Smith P 1999 *Nonlinear Ordinary Differential Equations* 3rd edn (Oxford: Oxford University Press)
[34] Chaikin P M and Lubensky T C 1995 *Principles of Condensed Matter* 1st edn (Cambridge: Cambridge University Press)